# Kinetic MHD Stability of Low-n Modes in Negative Triangularity Plasmas

Sunjae Lee[1], Jaebeom Cho[1], Oak Nelson[2], Carlos Paz-Soldan[2], J.-K. Park[1*]
[1]Seoul National University, Korea [2]Columbia University, USA
Email: satelite2517@snu.ac.kr
* jkpark@snu.ac.kr

***67th American Physical Society, Division of Plasma Physics, Long Beach, California, USA***

## Motivation

- Ideal MHD instabilities limit the stability of tokamak plasmas, but in **negative-triangularity (NT) plasmas** these limits can be different from positive-triangularity(PT) by **trapped-particle kinetic effects such as orbit anisotropy and resonant stabilization.**
- The influence of triangularity—particularly negative triangularity—on these **kinetic stabilization mechanisms** remains poorly understood and is systematically investigated in this study.

## Method

- Analysis is based on CHEASE code equilibria refined and modified from DIII-D discharges.
- Ideal, drift-kinetic, and full-kinetic stability analyses were carried out with **DCON and GPEC code suite.**

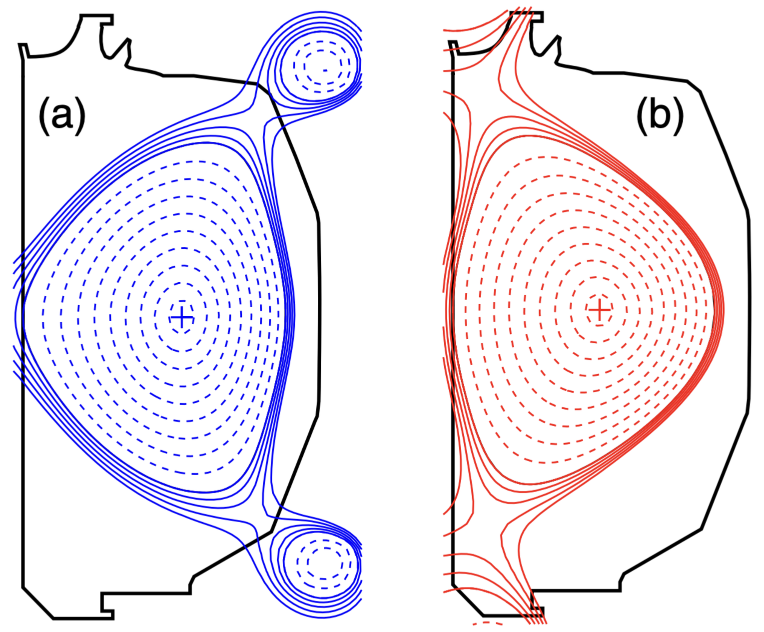


**Fig 1.** Reproduced from Austin et al., Phys. Rev. Lett. (2019) [3]

- **The kinetic MHD($\delta W_{kinetic}$)** perturbed potential energy is defined as[1][2]:

$$2\delta W_{kinetic} + i\frac{\tau_\varphi}{n} = 2\delta W_{Ideal} - \frac{2\pi\chi'}{M^2}\int d\psi d\varphi dE d\mu(\delta \mathcal{J}^* \delta f)$$

$$\delta f_{kls} = \sum_{\sigma\ell}\frac{1}{2\pi q}\frac{in\omega_{b,t}}{i[(\ell-\gamma nq)\omega_{b,t} - n\omega_p] - \nu}\frac{\partial f_M}{\partial \chi}\delta \mathcal{J}_{\sigma\ell} \quad (\delta\mathcal{J}_{\sigma\ell} = action\ variation$$

$$, \quad \omega_E \equiv electric\ precession\ frequency, \omega_B \equiv magnetic\ precession\ frequency,$$
$$\omega_p \equiv \omega_E + \omega_B = orbit - averaged\ precession\ frequency, \gamma = 1(0)\ for\ passing\ (trapped)\ particles)$$

- Due to dissipation breaking the energy principle, $\delta W_{kinetic} > 0$ is not a necessary but still a sufficient condition for stability.

$$\delta W_{kinetic} + \left(\frac{1-c}{c}\right)\frac{\tau_\varphi^2}{4n^2\delta W_L} < 0 \ (c: \text{plasma wall coupling})$$

- **The Kruskal–Oberman (KO) model** captures kinetic energy on fast MHD time scales, neglecting drift and collisions[4]: $\delta f_{ko} = -\frac{\omega_b}{2\pi T} f_M \delta \mathcal{J}$
- **The Chew–Goldberger–Low (CGL) model** describes a double-adiabatic pressure response that emerges as $\omega_E \to \infty$, suppressing orbit-resonant effects[5]: $\delta f_{cgl} = \lim_{\omega_E \to \infty} \delta f_{kls}$

## $n = 1$ Kinetic Stability

- Stability limits for the $n = 1$ mode were computed across triangularities using Ideal MHD, KO model, full kinetic, and CGL model in fig2.
- Generally, $\boldsymbol{\delta W_{Ideal} \le \delta W_{KO} \le \delta W_{kinetic} \le \delta W_{CGL}}$ is found as expected.
- NT showed a stronger **kinetic stabilizing effect.**
- Since the trapped particles satisfying the bounce-harmonic resonance condition ($\ell\omega_{b,t} - n\omega_p \approx 0$), shown in Fig. 3, strongly affect the kinetic-MHD response, we perform a bounce-harmonic scan to quantify this effect [6].
- As in Fig. 4, the bounce-harmonic scan indicates that $\delta W$ in NT converges much more slowly than in PT, demonstrating stronger trapped-particle coupling through higher-order harmonics.

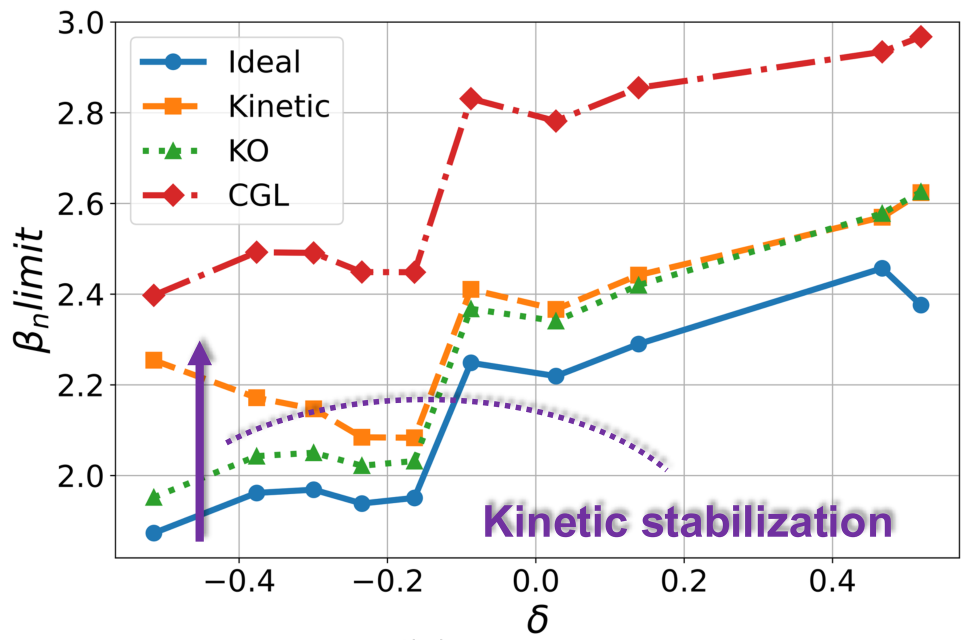


**Fig 2.** Stability limit $\beta_n^{limit}$ versus $\delta$, obtained from Ideal, Kinetic, KO model, and CGL models.

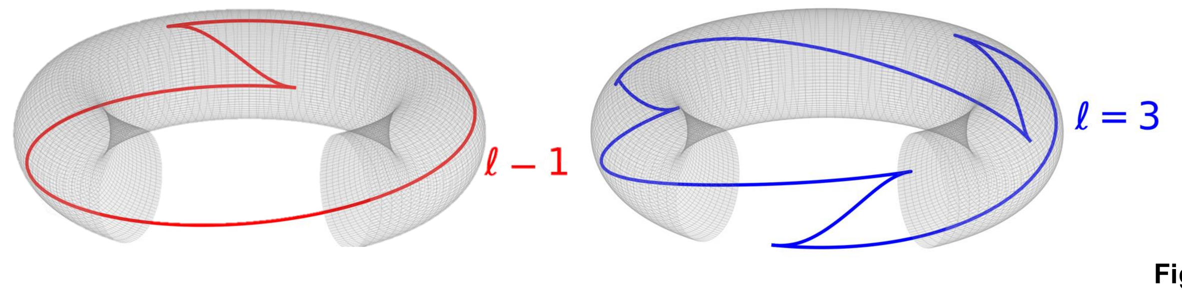


**Fig 3.** Particle trajectory of bounce harmonic resonance $(l, n) = (1,1), (l, n) = (1,3)$

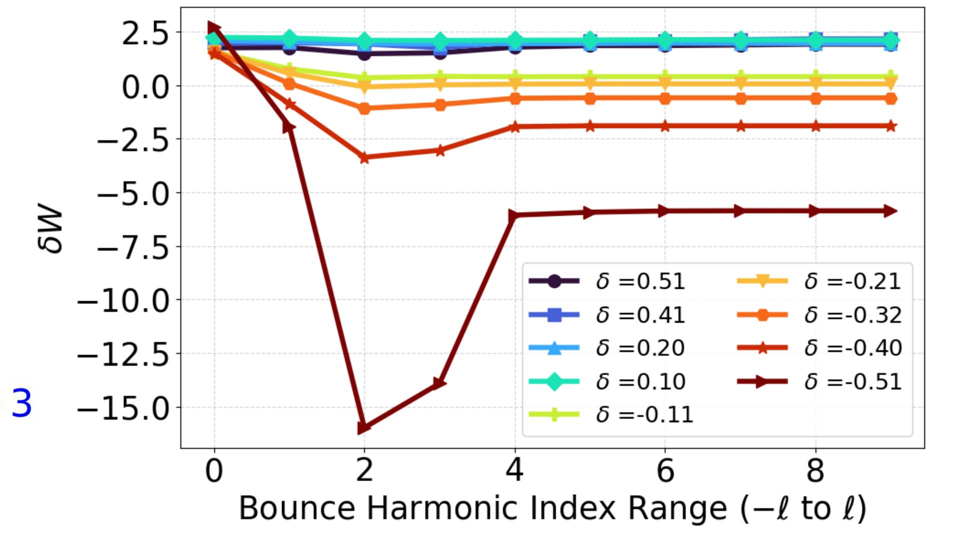


**Fig 4.** $\delta W$ convergence with bounce harmonics for various triangularities, showing strong trapped-particle effects at high negative $\delta$.

## Low $n$ Kinetic Stability

- **Full kinetic MHD analysis** including both ion and electron responses was performed. Direct-type equilibria were used for $n = 1–2$, and inverse-type for $n > 2$ to improve numerical precision.
- In **PT**, $n = 1–4$ becomes unstable as $\beta_n$ increases until hitting second stability regime, whereas in **NT** plasmas, ideal and drift-kinetic analyses still show $n > 1$ instabilities, but the full kinetic response completely stabilizes all $n > 1$ modes.
- $\delta W > 0$ means equilibrium is stable and $\delta W < 0$means unstable.

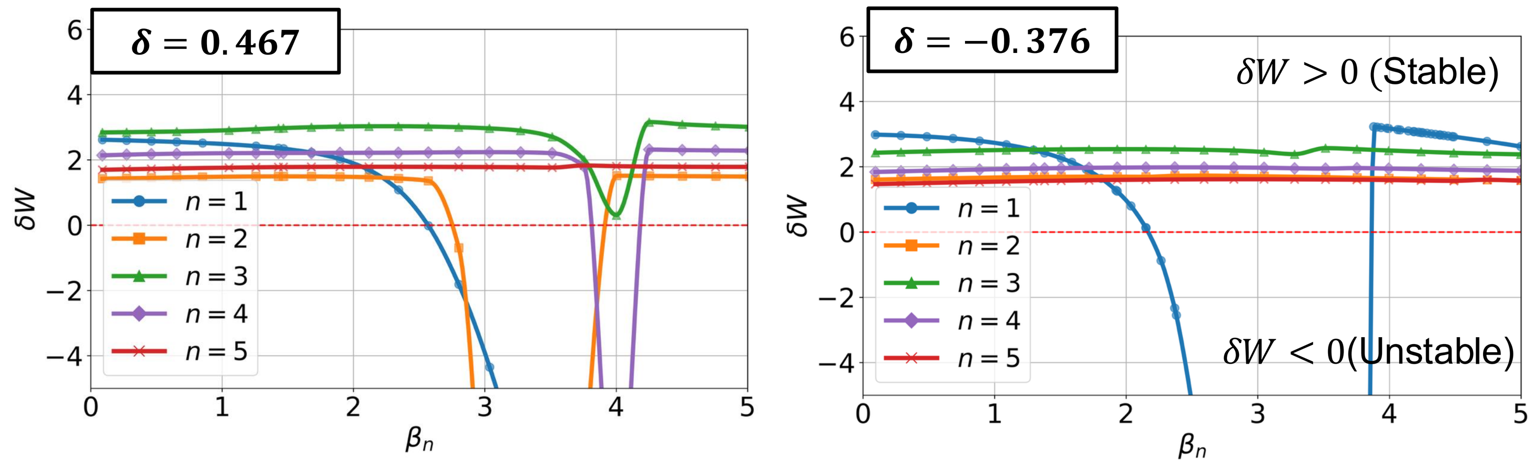


**Fig 5.** Perturbed potential energy $\delta W$ for toroidal modes $n = 1–5$ from full kinetic MHD analysis across $\beta_n$ scan.

## Low $n$ Second Stability Region

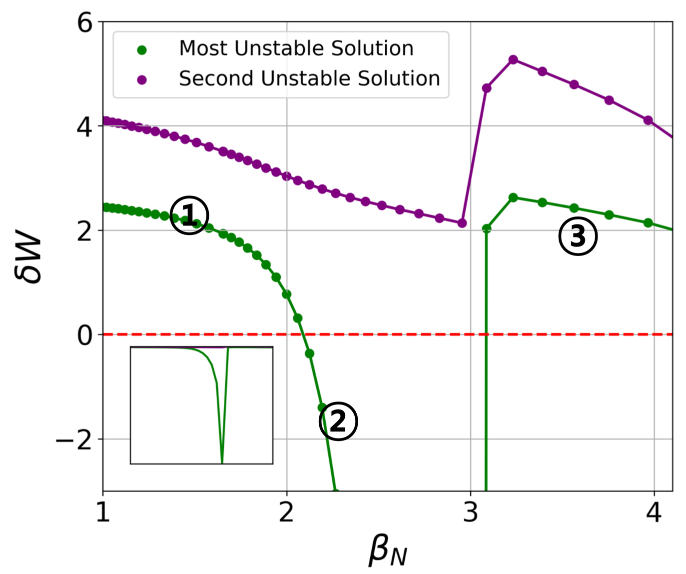


**Fig. 6.** $\delta W$calculated in most unstable solution and second unstable solution with Ideal-MHD across$\beta_n$

- In NT, the $(m, n) = (2,1)$ mode becomes unstable at lower $\beta_n$, consistent with NT's reduced stability limit. Beyond a certain point, however, only in NT does the $\boldsymbol{m = 2}$ **kink-like structure disappear, marking the onset of a second stability regime.**
- **The destabilizing $\boldsymbol{K}$ term** of $\delta W$, based on a simplified energy principal equation [7]:

$$\delta W_F = \frac{1}{2}\int\left[\frac{|\vec{C}|^2}{\mu_0} + \gamma p|\vec{\nabla}\cdot\vec{\xi}|^2 - K(\overrightarrow{\xi_\perp}\cdot\hat{n})^2\right]dx^3$$

$$(\overrightarrow{C} \equiv \vec{Q} + (\xi_\perp\cdot\hat{n})(\mu_0\vec{j}\times\hat{n}) = (effective\ perturbed\ field),$$

$$K \equiv 2(\vec{j}\times\hat{n})\cdot(\vec{B}\cdot\vec{\nabla}) = |\vec{\nabla}\psi|^2\left(\sigma S + \frac{\sigma^2 B^2}{|\vec{\nabla}\psi|^2} + \frac{2p'\kappa^\psi}{|\vec{\nabla}\psi|^2}\right), S = \text{shear},\ \sigma = \vec{j}\cdot\frac{\vec{B}}{B^2})$$

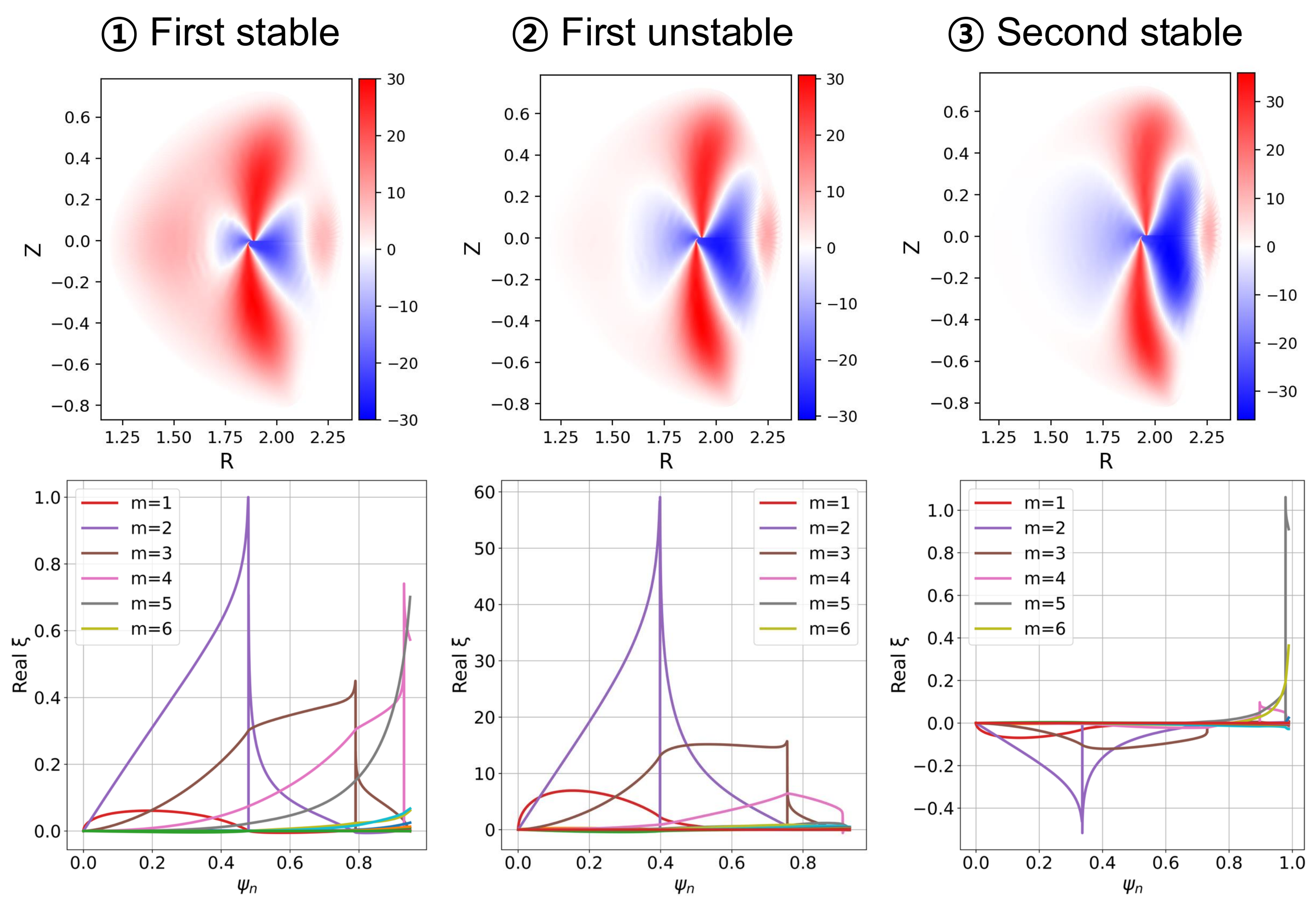


**Fig. 7.** Ideal-MHD mode structures across $\beta_n$ and K in the poloidal plane. (Red = unstable, blue = stable.)

- For low-n modes, a second-stability regime appears to emerge due to **magnetic shear**. This behavior may be influenced by the combined effects of negative shear and the **Shafranov shift**, with NT plasmas generally exhibiting a larger Shafranov shift [8].
- As shown in Fig. 7, stronger negative shear makes the $K$ term in the energy principle more negative.

*Note: The infinite-n ballooning mode was examined while maintaining the NT L-mode profile to isolate the effect of core pressure steepness. Under ideal MHD, instability persists even within this second stability regime. Future work will extend this analysis to include kinetic effects and construct a full stability map incorporating their responses.

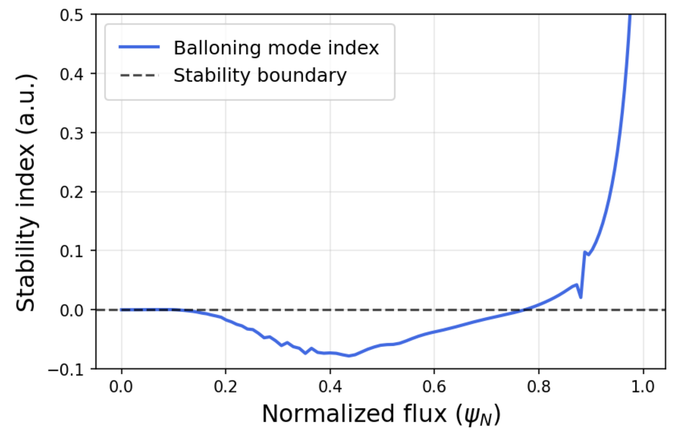


**Fig 8.** Infinite ballooning mode stability analysis results in this second stability region

## References

[1] J.-K. Park et al., Phys. Plasmas 23, 072505 (2016).
[2] J.-K. Park et al., Phys. Plasmas 24, 032505 (2017).
[3] Austin et al., Phys. Rev. Lett. 122, 115001 (2019)
[4] M. D. Kruskal and C. R. Oberman, Phys. Fluids 1, 275 (1958).
[5] J. P. Freidberg, Ideal MHD, Cambridge University Press (2014).
[6] J.K. Park et al., Phys. Rev. Lett. 102, 065002 (2009)
[7] I. B. Bernstein et al. Proc. R. Soc. London Ser. A 244, 17 (1958).
[6] Junhyuk Song et al 2021 Nucl. Fusion 61 096033

This work was supported by the National Research Foundation of Korea (NRF) grant funded by the Korea government (MSIT) Nos. RS-2023-00281276, by the U.S. Department of Energy under contract number DE-AC02-09CH11466, and supported by US DOE under DE-FC02-04ER54698